Charge Transport Parameters and Structural and Electronic Properties of Octathio[8]circulene and Its Plate-like Derivatives

Godefroid Gahungu,[†,‡] Jingping Zhang,*[,†] and Thaddée Barancira[§]

Faculty of Chemistry, Northeast Normal University, Changchun 130024, China, Département de Chimie, Université du Burundi, Bujumbura, BP 2700 Burundi, and Département de Physique, Université du Burundi, Bujumbura, BP 2700 Burundi

Received: June 5, 2008; Revised Manuscript Received: October 26, 2008

The first fully heterocyclic circulene very recently isolated, $C_{16}S_8$, was studied by means of high accurate methods, allowing reliable predictions and interpretations of the structural and electronic properties of organic molecules bearing sulfur and selenium atoms. The changes induced by the oxidation process and the S/Se substitution on some of its properties and the infrared (IR) spectra were analyzed, allowing a comprehensive assignment of the bands observed in the case of $C_{16}S_8$. The results confirmed the planarity and a large surface area of $C_{16}S_8$, which remain in $C_{16}S_4Se_4$ and $C_{16}Se_4$ derivatives, favoring their use for H_2 adsorption. The molecules were shown to have a strong aromatic character, while the IR spectrum of $C_{16}S_8$ was elucidated, toward its possible application for a better understanding of the new class of materials; the IR signal associated to the asymmetric stretching of the C═C bonds can be used as a structural signature to identify the neutral from the radical forms whose structural planarity was found to resist against the oxidation process. Some of the electronic and physical properties characterizing good electron-donating (ED) and charge-transporting (CT) capacity such as the frontier molecular orbital energies (E_{HOMO}, E_{LUMO}), the ionization potential (IP), and the reorganization energy (λ_h/λ_e for hole/electron) were calculated and the influence of the cyclic structure of $C_{16}S_8$ on them discussed. $C_{16}S_8$, $C_{16}S_4Se_4$, and $C_{16}Se_4$ were found to display a comparable/much lower λ_h and higher IP and E_{LUMO} than those for some of the already well-known field-effect transistors (FET) materials such as pentacene, anthracene, and DT-TTF; further investigation for this issue is strongly recommended.

1. Introduction

Organosulfur compounds display important electronic properties.[1] Thus, molecules like tetrathiafulvalenes and π-conjugated oligothiophenes are extensively used in light-emitting devices,[2] thin-film transistors,[3] and other applications.[4] Indeed, since the discovery of the first organic metal tetrathiafulvalene-7,7′,8,8′-tetracyanoquinodimethane (TTF-TCNQ) over 30 years ago,[5] tetrathiafulvalene (TTF) and its derivatives have been successfully used as building blocks for charge transfer salts, giving rise to a multitude of organic conductors and superconductors, as well as for the preparation of a wide range of molecular materials.[6] In the research field of organic field-effect transistors (OFETs),[7] thiophene oligomers[8] and acene molecules[9] have been extensively studied for over 20 years. With eight thiophene rings, octathio[8]circulene ($C_{16}S_8$) can be considered as a thiophene oligomer with a special cyclic structure, which differentiates it from the commonly studied thiophene oligomers. Popularly called sulflower, the molecule was the first fully heterocyclic circulene very recently synthesized and studied by Chernichenko et al.[10] The extremely close packing of the molecules in the solid state suggests strong intermolecular interaction both within layers and between adjacent layers.[10] Such interactions should be favorable for its future use as an electron donor in materials science applications. $C_{16}S_8$ was then considered as the first representative of a novel class of heterocyclic circulenes displaying a high structural stability, illustrating a possible development of an efficient synthetic methodology, which should be applicable to the new families of Se-, Te-, N-, and P-containing heterocyclic circulenes, with the success in the preparation of a mixed thiophene−selenophene circulene ($C_{16}S_4Se_4$) being announced already.

Since the synthesis of $C_{16}S_8$, only one year ago, a theoretical investigation has been reported, showing that because of its planar structure, the molecule can adsorb up to 10 hydrogen molecules.[11] The favorable mode of interaction was found to occur along the centers of mass of the alternate thiophene ring and the H_2 molecule, oriented vertically above and below, at a distance of 3.2 Å.[11] The nature of interactions between the molecule and the hydrogen molecules is physical adsorption, and the moderate binding energy for this material suggested that potential hydrogen-storage devices can be constructed by using this molecule.[6] Currently, nothing is known for $C_{16}S_4Se_4$, and even for $C_{16}S_8$, many of its properties are still unknown.

Electron Spin Resonance (ESR) investigations revealed the presence of a paramagnetic species that displays a broad singlet in the ESR spectrum (g factor: 2.008), [10] which most likely corresponds to the radical cation of $C_{16}S_8$. If this is the case, redox properties can be reasonably obtained from the molecule. For example, TTF undergoes a two-step, fully reversible oxidation, leading successively to the radical cation and the dication for well-separated, low values of the applied potential. On the basis of this property, many derivatives have been synthesized, and turned to become versatile building blocks, finding widespread use in the design of novel materials and supramolecular structures such as cation sensors, liquid crystals, molecular electronic switches and shuttles, and redox poly-

* Corresponding author. Fax: (+) 86-431-85684937. Phone: (+) 86-431-85099372. E-mail: zhangjingping66@yahoo.com.cn.
† Northeast Normal University.
‡ Département de Chimie, Université du Burundi.
§ Département de Physique, Université du Burundi.

10.1021/jp804986b CCC: $40.75
Published on Web 12/10/2008

mers.[12−16] It becomes thus interesting to know more about the cationic form, for which no other result has been reported so far. To obtain a better understanding of the redox properties of $C_{16}S_8$ derivatives and related compounds, it is of prime importance to elucidate the relationship between the structural properties and the electrochemical behavior of their oxidation products.

In this study, one of our main aims was to evaluate the electron-donating (ED) strength and charge-transport (CT) performance of $C_{16}S_8$ and some of its plate-like derivatives, including the thiophene−selenophene circulene ($C_{16}S_4Se_4$) whose synthesis was announced,[11] compared to some of the well-known ED and CT materials. For a good understanding of the influence of the cyclic structure, the linear homologue of $C_{16}S_8$, the octathienoacene (**8T**) having the same number of thiophene rings is considered. Second, we tried to investigate the oxidation products, a special emphasis being given to the radical $C_{16}S_8^+$ which, although not yet well characterized, was anyway identified experimentally. Finally, to provide some useful data for experimentalists in the development and a good understanding of the new class of materials, infrared spectra are discussed and a useful link to their use in the characterization of these compounds established. In this way, we intend to give our contribution to a good understanding and development of this new family of compounds whose many properties and characterization are still lacking.

2. Computational Strategy and Details

All the calculations were carried out within the density functional theory (DFT) approach, using the B03 revision of the GAUSSIAN 03 program package.[17] The atomic orbitals contributions to the molecular orbitals are analyzed by using the VModes 7.1 program.[18] Three functionals including the PBE1PBE (also called PBE0),[19] B3LYP,[20] and B3P86[21] were used with the 6-31G(d,p)[22] basis set. Both the PBE0 and B3P86 functionals are recognized to provide reliable predictions and interpretations of the molecular geometries, electronic properties,[23] and vibrational frequencies for sulfur and selenium compounds in good agreement with experimental data for organic molecules bearing sulfur and selenium atoms.[24] The radical cations and anions were treated as open-shell systems and were computed by using spin-unrestricted DFT wave functions (UB3P86 and UPBE0). The calculated harmonic vibrational frequencies were scaled down uniformly by a factor of 0.96, as suggested by Scott and Radom.[25] For the sake of comparison, already well-known charge transport materials (like pentacene[26] and dithiophene−tetrathiafulvalene (DT-TTF)[27]) were considered. In a first step, the geometry optimization was performed for both the neutral and ionic forms, using PBE0/6-31G(d,p). The ions were treated as open-shell systems, using the spin-unrestricted (UPBE0) approach. The reorganization energy λ_{reorg} (λ_h/λ_e for hole/electron) corresponds to the sum of geometry relaxation energies upon going from the neutral state geometry to the charged state geometry and vice versa. The geometry relaxation energies upon vertical transition from the neutral state to a charged state and vice versa ($\lambda_{rel}^{(1)}$ and $\lambda_{rel}^{(2)}$) are given by eqs 1 and 2.

$$\lambda_{rel}^{(1)} = E^{(1)}(M) - E^{0}(M) \quad (1)$$

$$\lambda_{rel}^{(2)} = E^{(1)}(M^{+/-\bullet}) - E^{0}(M^{+/-\bullet}) \quad (2)$$

Here, $E^0(M)$ and $E^0(M^{+/-\bullet})$ are the ground state energy of the neutral state and the energy of the considered cation/anion state, respectively, $E^{(1)}(M)$ is the energy of the neutral molecule at the optimal cation/anion geometry, and $E^{(1)}(M^{+/-\bullet})$ is the energy of the cation/anion state at the optimal geometry of the neutral molecule. A very good agreement was obtained with the (U)PBE0/6−31G(d,p). It has been shown[28] that the DFT estimates of the reorganization energy depend significantly on the amount of "exact" Hartree−Fock exchange included in the hybrid functionals. Among the standard functionals, B3LYP provides the best description of relaxation processes in oligoacenes. Recently, the same functional was successfully used to calculate the charge transport parameters for thiophene oligomers.[29] For these reasons, B3LYP/6-31G** single point calculations were performed and all the parameters necessary for the calculation of λ_{reorg} recomputed.

TABLE 1: B3P86/6-31G Optimized Bond Lengths (in Å) for $C_{16}S_8$, $C_{16}S_4Se_4$, and $C_{16}Se_8$ (See Labels in Scheme *1*)**

	$C_{16}S_8$		$C_{16}S_4Se_4$		$C_{16}Se_8$
bond	calcd[a]	exptl[b]	thio[c]	seleno[d]	seleno[d]
a	1.418	1.417	1.429	1.431	1.442
b	1.378	1.383	1.383	1.383	1.386
c	1.755	1.765	1.737	1.870	1.853
d	1.755	1.761	1.737	1.870	1.853
SA[e]	41.8		42.9		44.8

[a] Calculated. [b] Averaged experimental values based on the X-ray structure taken from CCDC No. 699788 (see ref 10). [c] Thiophene ring. [d] Selenophene ring. [e] Surface area (in Å^2).

3. Results and Discussion

3.1. Molecular Features. The discovery of $C_{16}S_8$ being no more than one year old, theoretical investigations on it are still rare from the literature. However, the two reported works about it are consistent with a planar or nearly planar structure. In our calculation both the C_1 and D_{8h} symmetries were considered. Both the B3P86 and PBE0 results are consistent with the planarity of the $C_{16}S_8$, and its preservation through the S/Se substitution. Comparing the C_1 to the D_{8h} geometries, very negligible differences were detected in the optimized parameters of both $C_{16}S_8$ and $C_{16}Se_8$, demonstrating the anticipated high symmetry of $C_{16}S_8$.[10,11] In comparison with the crystal structure,[10] a relatively significant difference was detected in the dihedral angles involving the S atom. We ascribe this to the solid-state effects, which are not taken into account in this study. From the bond lengths and angles viewpoint, however, an excellent agreement is observed (Table 1), implying that no profound alteration is induced by the solid state effect on the single molecule geometry. Apart from its very appealing chemical structure, $C_{16}S_8$ has a very large surface area, and coupled with its planar structure that ensures equal activity on either surface, it should be capable of adsorbing small molecules such as H_2. The surface area is even more enlarged by the S/Se substitution and thus was found in the increasing order $C_{16}S_8$ (∼41 Å^2) < $C_{16}S_4Se_4$ (∼43 Å^2) < $C_{16}Se_8$ (∼45 Å^2). Also, as $C_{16}S_8$, $C_{16}Se_8$, and $C_{16}S_4Se_4$ should be capable of absorbing small molecules, the planar structure, as a consequence of the presence of the S/Se atoms in $C_{16}Se_8$ and $C_{16}S_4Se_4$, should ensure similar activity of both the top and bottom surfaces of the rings.

In comparison with the neutral species, no significant geometrical changes are detected in the mono- and dicationic species. Indeed, both of the two positively charged forms are found to preserve the planar or nearly planar geometries with at most 0.018 Å and less than 2° of changes in bond lengths and angles. In the anionic species, however, the magnitude of the structural change depends on both the degree of S/Se

SCHEME 1: Chemical Structures of the Molecules Studied

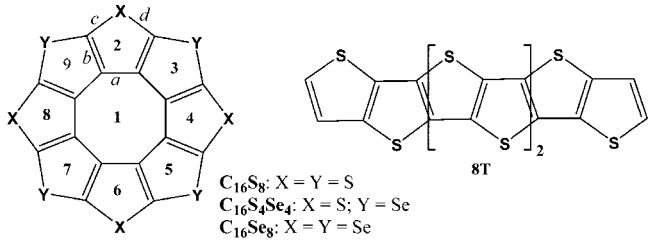

substitution and the charge. In $C_{16}S_8$, the anion shows a twist angle (θ) of ~10°, which is decreased to ~5.3° in $C_{16}S_4Se_4$, and ~0.0° in $C_{16}Se_8$, i.e., θ decreases in the order $C_{16}S_8^-$ > $C_{16}S_4Se_4^-$ > $C_{16}Se_8^-$. Figure 1 compares the oxidation and reduction products to the neutral $C_{16}S_8$.

By turning back to the geometric relaxation upon oxidation or reduction of an isolated $C_{16}S_8$, the C−C and C═C bonds undergo geometric changes to a greater extent in the cationic state than in the anionic state; the bond relaxations occur over the entire molecule and are more pronounced in rings 3, 4, 5, and 6. In Figure 2, we summarize the calculated variations in bond lengths for the different oxidation states of $C_{16}S_8$ (upon the redox process). For the C−S bond, the geometric relaxations are more pronounced in 3, 5, 7, and 9 and occur predominantly upon oxidation (as we will see below in section 3.3, the wave functions of the highest occupied molecular orbital (HOMO) have nodes on the sulfur atoms); the weak geometric changes in the cationic state are localized on the rings 2, 4, 6, and 8. Interestingly, a careful analysis of the structural changes as summarized in Figure 2 reveals a symmetry break from the D_{8h} to C_{2v} upon oxidation and to C_{4v} upon reduction. The same conclusion about symmetry can also be drawn from the Mulliken charge analysis as shown in Figure 3.

As an indicator of aromaticity, which is a useful criterion to judge the nature of a given heterocycle, the Nuclear Independent Chemical Shift (NICS)[30,31] values at the ring centers were calculated. To reveal the individual effect of the cyclic special structure and the S atoms, and for a good understanding of the structural aspect, a linear oligomer, the **8T** having the same number of thiophene rings, and the organic homologue ($C_{24}H_{16}$) of $C_{16}S_8$ were considered. From the results plotted in Figure 4, it becomes clear that $C_{24}H_{16}$ is of nonaromatic character (ca. 0 < NICS < 2.5), while $C_{16}S_8$ (ca. −9.7, except for the eight-membered ring) are of aromatic character. From the same results, it can be found that the S/Se substitution (see $C_{16}S_4Se_4$ and $C_{16}Se_8$) only slightly weakens the aromaticity. The eight-membered ring is found to be nonaromatic in $C_{24}H_{16}$, whose NICS value is between 0.2 and 0.3, with an antiaromatic tendency in $C_{16}S_8$, $C_{16}S_4Se_4$, and $C_{16}Se_8$, with NICS values between 5 and 5.7. In comparison with **8T**, the five-membered ring in $C_{16}S_8$ appears to be more aromatic except for the peripheral rings. From the computed NICS values, the thiophene rings within $C_{16}S_8$ display a strong aromatic character, which remains even upon reduction, but altered upon oxidation. The eight-membered ring displays an antiaromatic character in the neutral form, which is even more reinforced in the anionic

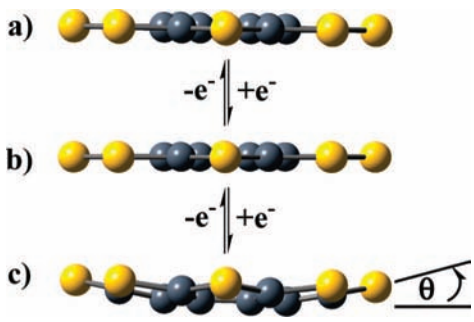

Figure 1. B3P86/6-31G(d,p) minimum energy conformations predicted for (a) $C_{16}S_8^+$, (b) $C_{16}S_8$, and (c) $C_{16}S_8^-$.

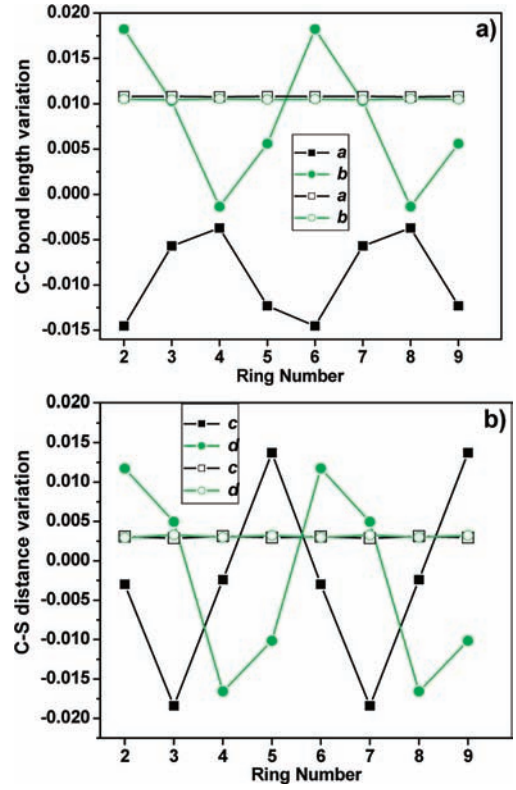

Figure 2. Calculated (a) C−C and (b) C−S bond length variations isolated for different oxidation states. Closed and opened symbols are used for oxidation and reduction, respectively (see Scheme 1 for definition of the parameters).

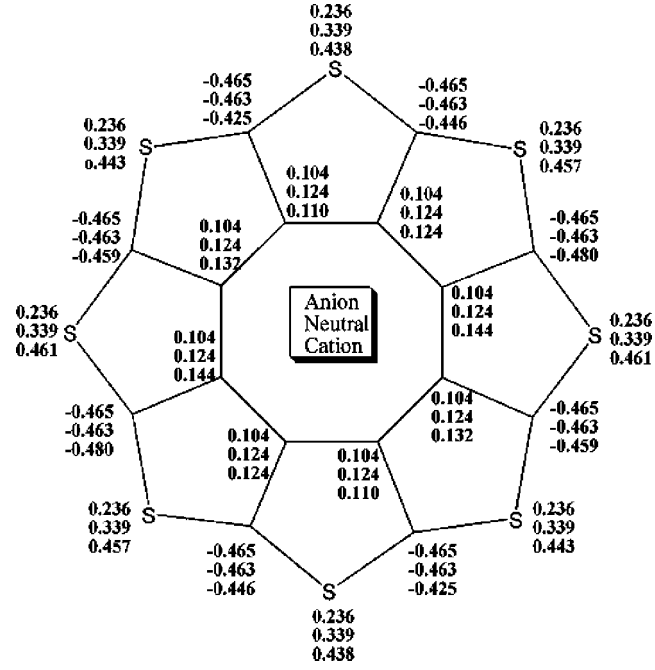

Figure 3. Mulliken (net) atomic charges (in e⁻) calculated for $C_{16}S_8$ (D_{8h}), $C_{16}S_8^+$ (nearly C_{2h}), and $C_{16}S_8^-$ (nearly C_{4v}) at the B3P86/6-31G** level.

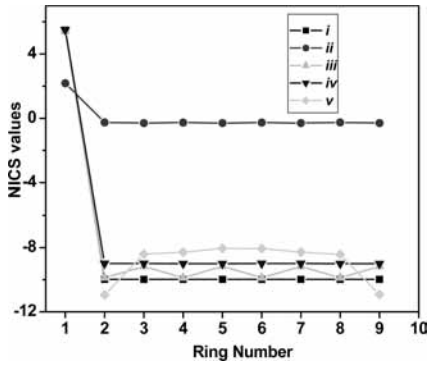

Figure 4. Computed NICS values of $C_{16}S_8$, $C_{24}H_{16}$, $C_{16}S_4Se_4$, $C_{16}Se_8$, and **8T** (labeled as $i-v$ respectively; see Scheme 1 for the labels of the rings).

species (NICS values not shown), while nonaromatic in the cationic forms. It was observed that the S/Se substitution slightly weakens the aromatic and antiaromatic character without any perturbation in the trend described above. Both the B3P86 and PBE0 are consistent with this feature. This result is found to be in agreement with a previous report (based on various criteria),[32] according to which selenophene was found to be less aromatic than thiophene. More details about the explanations (one of the explanations is relative to the fact that, compared to sulfur, selenium heteroatoms have a destabilizing effect, owing to the larger covalent radius, hence diminished p-orbital overlap, and higher propensity toward oxidation) can be found in the work by Alexandru and co-workers.[32] From the structural viewpoint, one of the direct consequences of the S/Se substitution is the longer C−Se than C−S bond, reinforcing the planarity and thus the surface area of the molecule stated in the fist paragraph of this section. In addition, the substitution preserves the resistance of the planarity of the molecular structure upon the redox process (θ increases in the order $C_{16}S_8^- > C_{16}S_4Se_4^- > C_{16}Se_8^-$).

3.2. Electronic Structure. From the frontier molecular orbitals (FMO) viewpoint, the general trend is that the HOMO (in $C_{16}S_8$, $C_{16}S_4Se_4$, and $C_{16}Se_8$) is predominantly composed of delocalized p_z atomic orbitals which are symmetric along the nodal plane, and this along with the planarity and highly symmetric molecular structure is also suggestive of aromaticity, which was also evidenced by the NICS values (ca. −9.7) in thiophene rings. For a good understanding of the influence of the cyclic structure on the electronic structure, we calculated and compared the molecular orbital contributions from sulfur and non-sulfur atoms to the FMOs for **8T** and $C_{16}S_8$. As shown from the results listed in Table 2 and Figure 5 (only for $C_{16}S_8$), the S atoms contribute more in the HOMO of $C_{16}S_8$ (∼46%) than that of **8T** (only ∼3%). Both B3P86/6-31(d,p) and PBE0/6-31(d,p) results reveal that the sulfur atoms only contribute for less than 3% to the HOMO in **8T**, while contributing for ∼46% to the HOMO in $C_{16}S_8$. For the LUMO, however, 37% and 31% of contributions from the sulfur atoms are revealed for $C_{16}S_8$ and **8T**, respectively. In general, the HOMO-1 appears to be mainly made up of sulfur atomic orbitals for **8T**, while in $C_{16}S_8$, only ∼8% of a difference in contributions is detected between sulfur and non-sulfur atoms. In reverse, the LUMO+1 of **8T** is mainly composed of atomic orbitals from the non-sulfur atoms, a relatively small difference (14%) in contributions for sulfur and non-sulfur atoms being detected in $C_{16}S_8$. These features suggest a significant difference in electronic properties between the two thiophene oligomers, implying that the special cyclic structure of $C_{16}S_8$ induces a significant influence from

TABLE 2: Molecular Orbital Contributions (%) from Sulfur (S) and Non-Sulfur (NS) Atoms to the 6 Frontier Molecular Orbitals (FMO) in $C_{16}S_8$ and Its Linear Homologue (8T)

	$C_{16}S_8$				**8T**			
	PBE0		B3P86		PBE0		B3P86	
FMO[a]	NS	S	NS	S	NS	S	NS	S
L+2	67.7	32.3	67.7	32.3	57.0	43.0	57.4	42.6
L+1	57.2	42.8	56.9	43.1	73.9	26.1	73.9	26.1
LUMO	62.7	37.3	62.6	37.4	68.8	31.2	68.8	31.2
HOMO	53.9	46.1	54.1	45.9	97.3	2.70	97.2	2.80
H−1	53.9	46.1	54.1	45.9	18.8	81.2	18.8	81.2
H−2	43.7	56.3	43.8	56.2	69.5	30.5	73.3	26.7

[a] H = HOMO and L = LUMO.

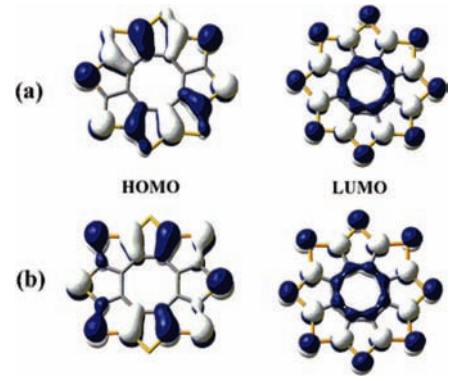

Figure 5. B3P86/6-31G(d,p) isodensity plots of HOMO and LUMO for (a) $C_{16}S_8$ and (b) $C_{16}S_4Se_4$.

TABLE 3: The FMO Energies E_{HOMO} and E_{LUMO} (eV) and Ionization Potential (IP in eV) at Different Levels of Theory

	B3P86/6-31G(d,p)			PBE0/6-31G(d,p)		
molecule	E_{HOMO}	E_{LUMO}	IP	E_{HOMO}	E_{LUMO}	IP
$C_{16}S_8$	−6.40	−1.68	7.67	−6.02	−0.94	7.17
$C_{16}S_4Se_4$	−6.19	−1.65	7.43	−5.80	−0.91	6.92
$C_{16}Se_8$	−6.02	−1.66	7.23	−5.61	−0.93	6.71
8T	−5.76	−2.50	6.82	−5.36	−1.78	6.29
TTF[a,b]	−5.19		6.74	−4.67	−0.75	6.16
TTM-TTF[a]	−5.57		6.65			
tetracene	−5.54	−2.76	6.95	−5.10	−2.03	6.38
pentacene	−5.28	−3.08	6.57	−4.83	−2.03	5.99
DT-TTF	−5.52	−1.79	6.69	−5.10	−1.01	6.33

[a] From ref 23a. [b] From ref 24.

the electronic structure viewpoint. One of the implications to this may be the relatively big difference in the E_{HOMO}, and thus the ionization potential (IP). In addition, as we know the changes induced by oxidation on the molecular geometry of $C_{16}S_8$ are easily understood by looking at the atomic orbital composition of the HOMO (Figure 5), which displays π-bonding interactions for the C=C bonds (except for two) and π-antibonding interactions for the C−S bonds. Thus, when electrons are removed from $C_{16}S_8$, the π-bonding bonds lengthen and the π-antibonding bonds shorten. Since S atoms do not contribute to the HOMO in **8T**, C−S bonds are expected to behave differently from those in $C_{16}S_8$ upon the redox process, resulting in a different contribution to the relaxation energy and to the reorganization energy.

From the FMO energies viewpoint (see Table 3), the results are consistent with the decrease of the E_{HOMO} through the substitution of S by Se in the increasing order of $C_{16}S_8 < C_{16}S_4Se_4 < C_{16}Se_8$, whereas the E_{LUMO} decreases slightly in the

order $C_{16}S_4Se_4$ > $C_{16}Se_8$ > $C_{16}S_8$. Going from sulfur to selenium, the energy of the p-orbitals increases, and consequently the HOMO (with a large amount of contribution of p-orbitals from S or/and Se) energies are increased, explaining the difference we observed in HOMO energy among $C_{16}S_8$ (−6.40 eV), $C_{16}S_4Se_4$ (−6.19 eV), and $C_{16}Se_8$ (−6.02 eV). Note that the change in the E_{FMO} is greater for the E_{HOMO} than the E_{LUMO} values. The ionization potentials (IP) calculations based on the energy differences indicate that **8T** is more easily oxidized than $C_{16}S_8$, $C_{16}S_4Se_4$, and $C_{16}S_8$; and $C_{16}Se_8$ is more easily oxidized than $C_{16}S_4Se_4$. A first theoretical approach to the energy required to extract an electron, i.e., to the ionization energy, can be obtained from the energy of the HOMO (Koopmans' theorem[33,34]). Since oxidation implies the extraction of an electron from the HOMO, more positive oxidation potentials are therefore to be expected for compounds with lower energy HOMOs. At the B3P86/6-31G** level, the HOMO of **8T** (−5.76 eV) is calculated at 0.64, 0.43, and 0.26 eV above the HOMOs of $C_{16}S_8$, $C_{16}S_4Se_4$, and $C_{16}Se_8$, thus supporting the increasing order in the IP values of **8T** < $C_{16}Se_8$ < $C_{16}S_4Se_4$ < $C_{16}S_8$, with the later being the least easily oxidized. Compared to the already well-known ED (such as TTF and TTM-TTF) and FET (such as pentacene, tetracene, and DT-TTF) compounds, $C_{16}S_8$ and its homologues are still less easily oxidized. To our knowledge, no experimental data are available in the literature for the ionization energy for any of these compounds.

3.3. Charge Transport Parameters. To obtain high electron mobility, organic semiconductors should have proper E_{LUMO} energy levels near the work function of electrodes.[35] To enhance the stability and obtain high hole mobilities in the thin films, fused aromatic rings or electron-deficient nitrogen heterocycles were introduced into the TTF skeleton,[36] to weaken the ED strength which makes the thin films labile to oxygen, resulting in poor FET performance.[37] From the results shown in Table 3, both sets of results (B3P86 and PBE0) are consistent with the fact that $C_{16}S_8$, $C_{16}S_4Se_4$, and $C_{16}Se_8$ fulfill the two requirements, compared to the materials taken as reference (also listed in this table). Indeed, one may find that the highest IP values (7.23−7.67 eV with B3P86, and 6.71−7.17 eV with PBE0) and the deepest HOMO (between −6.40 and − 6.02 eV with B3P86, −5.61 and −6.02 eV with PBE0) in energy correspond to them. This suggests a weaker ED strength compared to DT-TTF, pentacene, tetracene, TTF, and tetramethylthiofulvalene (TTM-TTF). Also, the results show a lifted LUMO in energy (−1.66 ± 0.02 eV with B3P86, and 0.99 ± 0.02 with PBE0) by up to 1.1 eV in the case of tetracene and pentacene. Assuming that CT can favor the FET use, these properties may allow improved performance.

To explain the high mobility of pentacene[38] and dithiophene−tetrathiafulvalene (DT-TTF)[39] transistors, previous studies have focused on the reorganization energy (λ_{reorg}) of the isolated molecules. A good agreement was found between our B3LYP λ_h values (0.092 ± 0.002 eV and 0.241 ± 0.002 eV for pentacene and DT-TTF, respectively), as shown in Table 4, and previously reported λ_h values (i.e., 0.098 eV[26,38] and 0.238 eV,[39,40] respectively). Since the crystal packing of $C_{16}S_8$[10] seems to be similar to those of DT-TTF[40] and pentacene, λ_{reorg} estimates can yield valuable predictions in the case of the compounds under study. With the reference of the λ_h for some of the well-studied hole-transport materials, this property was calculated by using the same methods for the molecules of interest, and a comparison was made. The results are summarized in Table 4. As shown, the B3LYP (PBE0) results provide λ_h values of 0.120 (0.133) eV for $C_{16}S_8$, 0.114 (0.138) eV for $C_{16}S_4Se_8$, 0.109 (0.118) eV for $C_{16}Se_8$, and 0.269 (0.275) eV for **8T**. For $C_{16}S_8$, $C_{16}S_4Se_4$, $C_{16}Se_8$, and **8T**, these results predict a much lower λ_h than that of DT-TTF (0.254/0.243 eV), and only slightly higher in comparison with that of pentacene (0.094/0.085 eV), implying a potential application of $C_{16}S_8$, $C_{16}S_4Se_8$, and $C_{16}Se_8$ as charge-transport materials. The consistency between B3P86- and B3LYP-based results suggests a certain reliability of the results reported herein, while for $C_{16}S_4Se_4$, λ_e is greater than λ_h, in agreement with the trend recently reported by Kim Eung-Gun et al. for a series of thienoacenes,[29] λ_e is smaller than λ_h for $C_{16}S_8$ and $C_{16}S_4Se_4$. Accordingly, we suggested further investigation on the OFET use of $C_{16}S_8$ and its S/Se substituted derivatives.

TABLE 4: Calculated Intramolecular Reorganization Energies (eV) for Hole (λ_h) and Electron (λ_e) in $C_{16}S_8$, $C_{16}S_4Se_4$, and $C_{16}S_8$ (for Comparison, λ_h Values for 8T, Tetracene, Pentacene, and DT-TTF Are Listed)

	λ_h				λ_e	
molecule	PBE0	B3P86	B3LYP[a]	B3LYP[b]	B3P86	B3LYP[b]
$C_{16}S_8$	0.133	0.125	0.120	0.126	0.420	0.399
$C_{16}S_4Se_4$	0.138	0.119	0.114	0.113	0.172	0.169
$C_{16}Se_8$	0.118	0.117	0.109	0.106		
8T	0.275	0.257	0.269	0.261	0.213	0.216
tetracene	0.118	0.100	0.115	0.112		
pantacene	0.085	0.077	0.094	0.091 (*0.098*)[c]		
DT-TTF	0.253	0.241	0.243	0.242 (*0.238*)[d]		

[a] PBE0/6-31G(d,p) geometries. [b] B3P86/6-31G(d,p) geometries. [c] Theoretical value from refs 26 and 38. [d] Theoretical value from refs 39 and 40.

3.4. Infrared Spectra. Infrared spectroscopy is a technique that allows the pinpointing of the structural properties in a molecule, which was demonstrated to return a vibrational spectroscopic signature for all the species appearing during the redox process in the cases of TTF and TTM-TTF.[24] Analyzing the IR spectra of these two compounds, DFT calculations of the frequency and structural changes induced by redox process were shown to be of important use in the understanding of corresponding properties.[24] The vibrational spectrum has been intensively and successively used in numerous investigations on oligothienoacenes,[41] oligothiophenes,[42] and thiophene- and selenophene-based heteroacenes.[43] In our studied cases, the IR spectra calculated for neutral and cationic species in the 400−1600 cm^{-1} range are displayed in Figures 6 and 8. For the sake of comparison, the spectrum of the neutral $C_{16}S_8$ in the frequency range of 1000−1600 cm^{-1} is displayed separately in Figure 8a because of the relative low intensity of the peaks calculated compared to those of the cationic species (Figure 8b). The neutral $C_{16}S_8$ presents three peaks at 1408, 947, and 492 cm^{-1} with calculated intensities (I) of 24, 87, and 24 and a very small peak at 1099 cm^{-1} (I = 1). The peak at 1408 cm^{-1} corresponds to the vibration mode shown in Figure 7d, which describes the symmetric stretching of the C=C double bonds. The peaks at 946 and 492 cm^{-1} correspond to the experimentally observed intense ones at 947 and 499 cm^{-1}, respectively,[10] characterizing the C−S bonds. As one may find, the agreement between these and the predicted values is excellent.

The neutral $C_{16}Se_8$ displays three intense peaks at 1353, 887, and 494 cm^{-1} which were assigned similarly to previous ones, in the case of $C_{16}S_8$. A careful analysis shows that, compared to $C_{16}S_8$, the peaks in $C_{16}Se_8$ correspond to a downshift of ∼55 and 59 cm^{-1} of the first two in the former. In the neutral

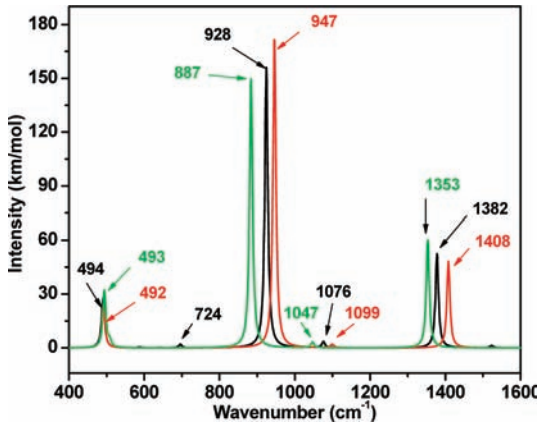

Figure 6. B3P86/6-31G(d,p) IR spectra of the neutral molecules: green, black, and red are used for $C_{16}Se_8$, $C_{16}S_4Se_4$, and $C_{16}S_8$, respectively.

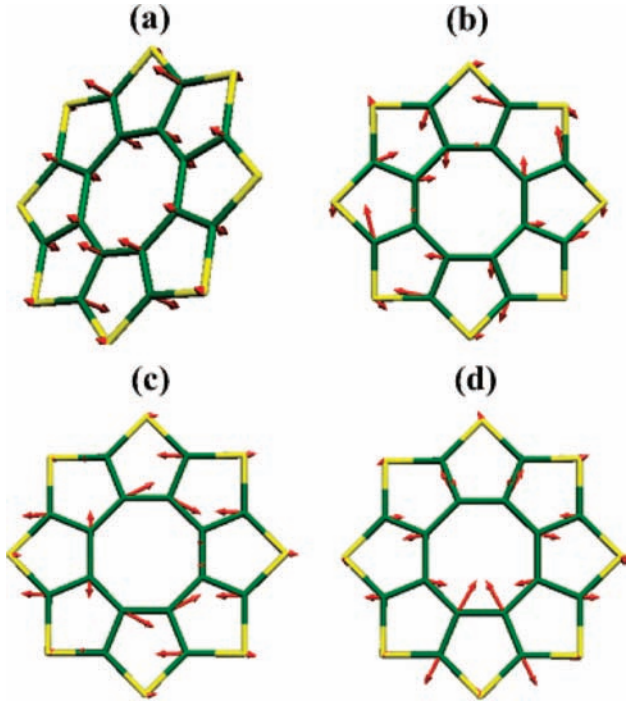

Figure 7. B3P86/6-31G** eigenvectors associated to the normal modes calculated at 492, 947, 1099, and 1408 cm^{-1} for neutral $C_{16}S_8$.

$C_{16}S_4Se_4$, the same situation is observed. The most intense three peaks (1382, 928, and 493 cm^{-1}) are predicted at wavenumber values between those for $C_{16}S_8$ and $C_{16}Se_8$.

Since the radical cation of $C_{16}S_8$ ($C_{16}S_8^+$) was experimentally detected, IR spectra analysis will concentrate on the cationic species. Here, we describe the influence of the redox process on the IR spectrum of the neutral form. In Figure 8b, we plot the IR spectra of $C_{16}S_8^+$ and $C_{16}S_8^{2+}$ in the frequency range of 1000−1700 cm^{-1}. This range was chosen since most of the interesting changes in the IR spectrum upon reduction were found in it. As one may find, more peaks appear in this range compared to the neutral form. For $C_{16}S_8^+$, the most intense peak corresponds to a double peak calculated at 1401 (I = 2268 km mol^{-1}) and 1423 cm^{-1} (I = 1207 km mol^{-1}) corresponding to asymmetric stretching of four of the eight C═C bonds. The peak at 1397 cm^{-1} originates in a set of asymmetric stretching of the other four bonds. The double peak at 1566 and 1584 cm^{-1} (I = 228 and 288, respectively) corresponds to the sets of vibrational modes associated to the C−C bending. The double

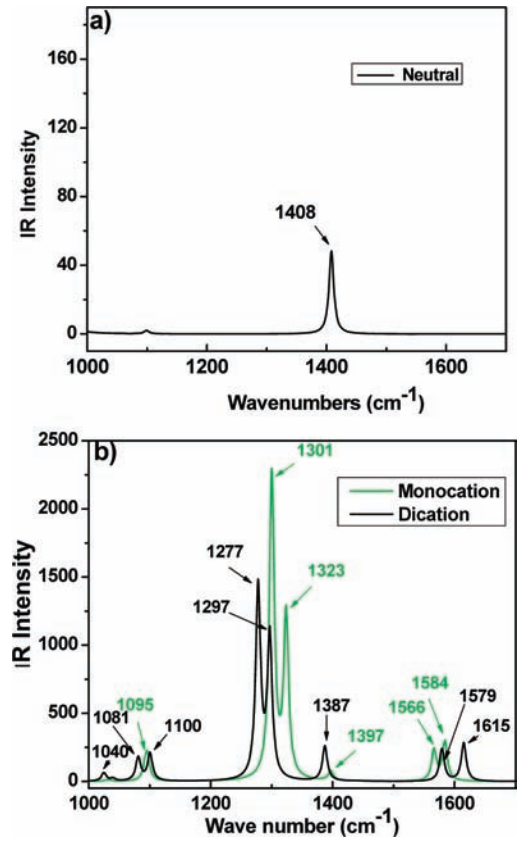

Figure 8. B3P86/6-31G(d,p) IR spectra for (a) the neutral $C_{16}S_8$ and (b) $C_{16}S_8^+$ and $C_{16}S_8^{2+}$ in the range of frequencies 1000−1600 cm^{-1}.

peak at 1092 and 1095 cm^{-1} (I = 63 and 186, respectively) corresponds to the sets of vibrational modes associated to C═C bending. Another doublepeak (not shown in the figure) appears at 918 and 928 cm^{-1}, which corresponds to the vibrational modes associated to the C−S bendings (wagging + rocking). The other double peak was calculated at 733 (and 735) cm^{-1}, which was assigned to the vibrational mode associated to asymmetric C═C stretching. Finally, in the same range, two peaks at 612 and 499 cm^{-1} were both being assigned to the C−S bending (out-of-plane and in-plane, respectively).

The calculated IR spectrum for $C_{16}S_8^{2+}$ shows nearly the same trend as the one discussed for the radical $C_{16}S_8^+$. The most intense double peak due to the asymmetric $\nu_{C=C}$ shifts down by ∼25 cm^{-1} to 1297 cm^{-1} and 1277 and cm^{-1} in comparison to 1323 and 1301 cm^{-1} predicted in the case of $C_{16}S_8^+$. In comparison with the neutral $C_{16}S_8$ ($\nu_{C=C}$ = 1408 cm^{-1}), this corresponds to a downshift of 101 and 131 cm^{-1}, a dramatic difference in intensity being also observed (see Figure 8 for details). The frequency downshift is due to the lengthening of the C═C bonds directly involved in the vibration (see Figure 2). The intensity increase is due to the electrical dipole moment induced by the asymmetric vibrational motion. The magnitude of the induced dipole strongly depends on the net charges supported by the vibrating atoms and is expected to increase with the oxidation state due to the increase in the atomic charges.

As a summary, theoretical calculations predict very low-intensity vibrations for neutral $C_{16}S_8$ compared with those obtained for the cation and the dication. The peak observed at 724 cm^{-1} was not found in our predictions and may be due to the experimental medium not being taken into account in the present investigation. However, all the others are predicted in

excellent accuracy, which gives credit to the computational approach. The vibrational band associated to the asymmetric stretching of the C═C bonds of $C_{16}S_8$ was shown to undergo a frequency downshift with oxidation. The corresponding bands can be used as a signature of the oxidation state of $C_{16}S_8$ and their high intensities may allow experimentalists to follow the oxidation process.

4. Concluding Remarks

The first fully heterocyclic circulene very recently isolated, $C_{16}S_8$, was studied by means of quantum chemical methods based on DFT-B3P86 and PBE0, allowing reliable predictions and interpretations of the structural and electronic properties of organic molecules bearing sulfur and selenium atoms. The changes induced by the oxidation process and the S/Se substitution on some properties and IR spectra were analyzed, allowing a comprehensive assignment of the bands observed in the case of $C_{16}S_8$. The results confirmed the planarity and a large surface area of $C_{16}S_8$, which remain in $C_{16}S_4Se_4$ and $C_{16}Se_4$, favoring their use for H_2 adsorption. The molecules were shown to have a strong aromatic character and the IR spectrum of $C_{16}S_8$ elucidated toward a possible application for a better understanding of the new class of materials; the IR signal associated to the asymmetric stretching of the C═C bonds can be used as a structural signature to identify the neutral from of the radical forms whose structural planarity was found to resist the oxidation process. Some of the electronic and physical properties characterizing good ED and CT capacity such as frontier molecular orbital energies (E_{HOMO}, E_{LUMO}), the IP, and the λ_h/λ_e (for hole/electron) were calculated and the influence of the cyclic geometry of $C_{16}S_8$ on them discussed. $C_{16}S_8$, $C_{16}S_4Se_4$, and $C_{16}Se_4$ were found to display a comparable/much lower λ_h and higher IP and E_{LUMO} than those for some of the already well-known FET materials such as pentacene, anthracene, and DT-TTF; further investigation for this issue is thus strongly recommended.

Acknowledgment. Financial support from the NSFC (Nos. 50873020, 20773022), the NCET-06-0321, and the NENU-STB-07-007 is gratefully acknowledged.

Supporting Information Available: Cartesian coordinates of the optimized geometries and a table containing optimized bond and corresponding variations in siolated sulflower upon oxidation. This material is available free of charge via the Internet at http://pubs.acs.org.

References and Notes

(1) Gingras, M.; Raimundo, J.-M.; Chabre, Y. M. *Angew. Chem., Int. Ed.* **2006**, *45*, 1686.

(2) Perepichka, I.; Perepichka, D.; Meng, H.; Wudl, F. *Adv. Mater.* **2005**, *17*, 2281.

(3) (a) Sun, Y.; Liu, Y.; Zhu, D. *J. Mater. Chem.* **2005**, *15*, 53. (b) Mas-Torrent, M.; Rovira, C. *J. Mater. Chem.* **2006**, *16*, 433.

(4) Barbarella, G.; Melucci, M.; Sotgiu, G. *Adv. Mater.* **2005**, *17*, 1581.

(5) Ferraris, J.; Cowan, D. O.; Walatka, V. V.; Perlstein, J. H. *J. Am. Chem. Soc.* **1973**, *95*, 948.

(6) Williams, J. M.; Ferraro, J. R.; Thorn, R. J.; Carlson, K. D.; Geiser, U.; Wang, H. H.; Kini, A. M.; Whangbo, M.-H. *Organic Superconductors (Including Fullerenes): Synthesis, Structure, Properties, and Theory*; Prentice Hall: Englewood Cliffs, NJ, 1992.

(7) (a) Facchetti, A.; Yoon, M.-H.; Stern, C. L.; Katz, H. E.; Marks, T. J. *Angew. Chem., Int. Ed.* **2003**, *42*, 3900. (b) Dimitrakopoulos, C. D.; Malenfant, P. R. L. *Adv. Mater.* **2002**, *14*, 99. (c) Moon, H.; Zeis, R.; Borkent, E. J.; Besnard, C.; Lovinger, A. J.; Siegrist, T.; Kloc, C.; Bao, Z. *J. Am. Chem. Soc.* **2004**, *126*, 15322.

(8) (a) Facchetti, A.; Letizia, J.; Yoon, M.-H.; Mushrush, M.; Katz, H. E.; Marks, T. J. *Chem. Mater.* **2004**, *16*, 4715. (b) Takimiya, K.; Kunugi, Y.; Konda, Y.; Ebata, H.; Toyoshima, Y.; Otsubo, T. *J. Am. Chem. Soc.* **2006**, *128*, 3044.

(9) (a) Payne, M. M.; Parkin, S. R.; Anthony, J. E.; Kuo, C.-C.; Jackson, T. N. *J. Am. Chem. Soc.* **2005**, *127*, 4986. (b) Tulevski, G. S.; Miao, Q.; Afzali, A.; Graham, T. O.; Kagan, C. R.; Nuckolls, C. *J. Am. Chem. Soc.* **2006**, *128*, 1788.

(10) Chernichenko, K. Y.; Sumerin, V. V.; Shpanchenko, R. V.; Balenkova, E. S.; Nenajdenko, V. G. *Angew. Chem, Int. Ed.* **2006**, *45*, 7367.

(11) Datta, A.; Pati, S. K. *J. Phys. Chem. C* **2007**, *111*, 4487.

(12) Jørgensen, T.; Hansen, T. K.; Becher, J. *Chem. Soc. Rev.* **1994**, *23*, 41.

(13) Bryce, R. *Adv. Mater.* **1999**, *11*, 11.

(14) Bryce, M. R. *J. Mater. Chem.* **2000**, *10*, 589.

(15) Nielsen, M. B.; Lomholt, C.; Becher, J. *Chem. Soc. Rev.* **2000**, *29*, 153.

(16) Segura, J. L.; Martin, N. *Angew. Chem., Int. Ed.* **2001**, *40*, 1372.

(17) Frisch, M. J.; Trucks, G. W.; Schlegel, H. B.; Scuseria, G. E.; Robb, M. A.; Cheeseman, J. R.; Montgomery J. A., Jr.; Vreven, T.; Kudin, K. N.; Burant, J. C.; Millam, J. M.; Iyengar, S. S.; Tomasi, J.; Barone, V.; Mennucci, B.; Cossi, M.; Scalmani, G.; Rega, N.; Petersson, G. A.; Nakatsuji, H.; Hada, M.; Ehara, M.; Toyota, K.; Fukuda, R.; Hasegawa, J.; Ishida, M.; Nakajima, T.; Honda, Y.; Kitao, O.; Nakai, H.; Klene, M.; Li, X.; Knox, J. E.; Hratchian, H. P.; Cross, J. B.; Bakken, V.; Adamo, C.; Jaramillo, J.; Gomperts, R.; Stratmann, R. E.; Yazyev, O.; Austin, A. J.; Cammi, R.; Pomelli, C.; Ochterski, J. W.; Ayala, P. Y.; Morokuma, K.; Voth, G. A.; Salvador, P.; Dannenberg, J. J.; Zakrzewski, V. G.; Dapprich, S.; Daniels, A. D.; Strain, M. C.; Farkas, O.; Malick, D. K.; Rabuck, A. D.; Raghavachari, K.; Foresman, J. B.; Ortiz, J. V.; Cui, Q.; Baboul, A. G.; Clifford, S.; Cioslowski, J.; Stefanov, B. B.; Liu, G.; Liashenko, A.; Piskorz, P.; Komaromi, I.; Martin, R. L.; Fox, D. J.; Keith, T.; Al-Laham, M. A.; Peng, C. Y.; Nanayakkara, A.; Challacombe, M.; Gill, P. M. W.; Johnson, B.; Chen, W.; Wong, M. W.; Gonzalez, C.; Pople, J. A. *GAUSSIAN 03*;Gaussian, Inc., Wallingford CT, 2004.

(18) Nemykin, V. N.; Basu, P. *VMOdes Program*, Revision A 7.2; University of Minnesota Duluth and Duquesne University, 2001, 2003, 2005.

(19) (a) Adamo, C.; Barone, V. *J. Chem. Phys.* **1999**, *110*, 6158. (b) Ernzerhof, M.; Scuseria, G. E. *J. Chem. Phys.* **1999**, *110*, 5029.

(20) (a) Becke, A. D. *Phys. Rev. A: At., Mol., Opt. Phys.* **1988**, *38*, 3098. (b) Lee, C.; Yang, W.; Parr, R. G. *Phys. Rev. B: Condens. Matter* **1988**, *37*, 785. (c) Stephens, P. J.; Devlin, F. J.; Chabalowski, C. F.; Frisch, M. J. *J. Phys. Chem.* **1994**, *98*, 11623.

(21) (a) Perdew, J. P. *Phys. Rev. B.* **1986**, *33*, 8822. (b) Becke, A. D. *J. Chem. Phys.* **1993**, *98*, 5648.

(22) (a) Hariharan, P. C.; Pople, J. A. *Mol. Phys.* **1974**, *27*, 209. (b) Gordon, M. S. *Chem. Phys. Lett.* **1980**, *76*, 163. (c) Frisch, M. J.; Pople, J. A.; Binkley, J. S. *J. Chem. Phys.* **1984**, *80*, 3265.

(23) (a) Gahungu, G.; Zhang, B.; Zhang., J. *J. Phys. Chem. C* **2007**, *111*, 4838. (b) Jacquemin, D.; Perpète, E. A. *Chem. Phys. Lett.* **2006**, *429*, 147. (c) Prpète, E. A.; Preat, J.; Andre, J. M.; Jacquemin, D. *J. Phys. Chem. A* **2006**, *110*, 5629.

(24) Wartelle, C.; Viruela, R.; Viruela, P. M.; Sauvage, F. X.; Salle, M.; Orti, E.; Levillain, E.; Le Derf, F. *Phys. Chem. Chem. Phys.* **2003**, *5*, 4672.

(25) Scott, A. P.; Radom, L. *J. Phys. Chem.* **1996**, *100*, 16502.

(26) (a) Dimitrakopoulos, C. D.; Malenfant, P. R. L. *Adv. Mater.* **2002**, *14*, 99. (b) Sun, Y.; Liu, Y.; Zhu, D. *J. Mater. Chem.* **2005**, *15*, 53. (c) Anthony, J. E. *Chem. Rev.* **2006**, *106*, 5028.

(27) Mas-Torrent, M.; Durkut, M.; Hadley, P.; Ribas, X.; Rovira, C. *J. Am. Chem. Soc.* **2004**, *126*, 984.

(28) Sánchez-Carrera, R. S.; Coropceanu, V.; daSilvaFilho, D. A.; Friedlein, R.; Osikowicz, W.; Murdey, R.; Suess, C.; Salaneck, W. R.; Brédas, J.-L. *J. Phys. Chem. B* **2006**, *110*, 18904.

(29) (a) Kim, E.-G.; Coropceanu, V.; Gruhn, N. E.; Sánchez-Carrera, R. S.; Snoeberger, R.; Matzger, A. J.; Brédas, J.-L. *J. Am. Chem. Soc.* **2007**, *129*, 13072. (b) Bromley, S. T.; Mas-Torrent, M.; Hadley, P.; Rovira, C. *J. Am. Chem. Soc.* **2004**, *126*, 6544.

(30) Schleye, P. v. R.; Maerker, C.; Dransfeld, A.; Jiao, H.; Hommes, N. J. R. v. E. *J. Am. Chem. Soc.* **1996**, *118*, 6317.

(31) Schleyer, P. v. R.; Manoharan, M.; Wang, Z.-X.; Kiran, B.; Jiao, H.; Puchta, R.; van Eikema Hammes, N. J. R. *Org. Lett.* **2001**, *3*, 2465.

(32) Alexandru, T. B.; Daniela, C. O.; Alan, R. K. *Chem. Rev.* **2004**, *104*, 2777.

(33) Koopmans, T. *Physica* **1934**, *1*, 104.

(34) Richards, W. G. *Int. J. Mass Spectrom. Ion Phys.* **1969**, *2*, 419.

(35) (a) Anthony, J. E.; Brooks, J. S.; Eaton, D. L.; Parkin, S. R. *J. Am. Chem. Soc.* **2001**, *123*, 9482. (b) Anthony, J. E.; Eaton, D. L.; Parkin, S. R. *Org. Lett.* **2002**, *4*, 15.

(36) Naraso, J.-I.; Nishida, J.; Ando, S.; Yamaguchi, J.; Itaka, K.; Koinuma, H.; Tada, H.; Tokito, S.; Yamashita, Y. *J. Am. Chem. Soc.* **2005**, *127*, 10142.

(37) (a) Noda, B.; Katsuhara, M.; Aoyagi, I.; Mori, T.; Taguchi, T.; Kambayashi, T.; Ishikawa, K.; Takezoe, H. *Chem. Lett.* **2005**, *34*, 392. (b)

Katsuhara, M.; Aoyagi, I.; Nakajima, H.; Mori, T.; Kambayashi, T.; Ofuji, M.; Takanishi, Y.; Ishikawa, K.; Takezoe, H.; Hosono, H. *Synth. Met.* **2005**, *149*, 219.

(38) Gruhn, N. E.; da Silva Filho, D. A.; Bill, T. G.; Malagoli, M.; Coropceanu, V.; Kahn, A.; Brédas, J.-L. *J. Am. Chem. Soc.* **2002**, *124*, 7918.

(39) Bromley, S. T.; Mas-Torrent, M.; Hadley, P.; Rovira, C. *J. Am. Chem. Soc.* **2004**, *126*, 6544.

(40) Mas-Torrent, M.; Hadley, P.; Bromley, S. T.; Ribas, X.; Tarre's, J.; Mas, M.; Molins, E.; Veciana, J.; Rovira, C. *J. Am. Chem. Soc.* **2004**, *126*, 8546.

(41) Osuna, R. M.; Zhang, X.; Matzger, A. J.; Hernández, V.; Teodomiro, J.; Navarrete, L *J. Phys. Chem. A* **2006**, *110*, 5058.

(42) Osuna, R. M.; Ortiz, R. P.; Hernández, V.; Teodomiro, J.; Navarrete, L.; Miyasaka, M.; Rajca, S.; Rajca, A.; Glaser, R. *J. Phys. Chem. C.* **2007**, *111*, 4854.

(43) Osuna, R. M.; Ortiz, R. P.; Okamoto, T.; Suzuki, Y.; Yamaguchi, S.; Hernandez, V.; Teodomiro, J.; Navarrete, L. *J. Phys. Chem. B.* **2007**, *111*, 7488.

JP804986B